

Volume Minimization of Current Type ACC with Rogowski Coil

Atsutoshi Okura
Dept. of Electrical, Electronics, and
Information Engineering
Nagaoka University of Technology
Niigata, Japan
s193118@stn.nagaokaut.ac.jp

Rintaro Kusui
Dept. of Electrical, Electronics, and
Information Engineering
Nagaoka University of Technology
Niigata, Japan
kusui@stn.nagaokaut.co.jp

Kodai Nishikawa
Dept. of Electrical, Electronics, and
Information Engineering
Nagaoka University of Technology
Niigata, Japan
knishikawa@stn.nagaokaut.co.jp

Masamichi Yamaguchi
Dept. of Electrical, Electronics, and
Information Engineering
Nagaoka University of Technology
Niigata, Japan
m_yamaguchi@stn.nagaokaut.ac.jp

Hiroki Watanabe
Dept. of Electrical, Electronics, and
Information Engineering
Nagaoka University of Technology
Niigata, Japan
hwatanabe@vos.nagaokaut.ac.jp

Jun-ichi Itoh
Dept. of Electrical, Electronics, and
Information Engineering
Nagaoka University of Technology
Niigata, Japan
itoh@vos.nagaokaut.ac.jp

Abstract— This paper proposes a current type active common-mode noise canceller (ACC) using a Rogowski coil for common-mode (CM) noise detection. The proposed method reduces the volume of a noise filter more than that of conventional methods. The Rogowski coil is designed based on CISPR standards for detecting the target noise reduction and the frequency band. The proposed ACC with the Rogowski coil is evaluated in the experiment. As a result, the conducted emission voltage is reduced by 39dB μ V.

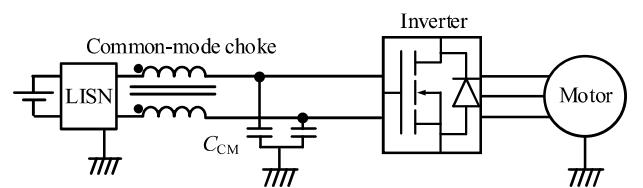
Keywords— wide-band-gap semiconductor, common-mode current, passive filter, active common-mode noise canceller

I. INTRODUCTION

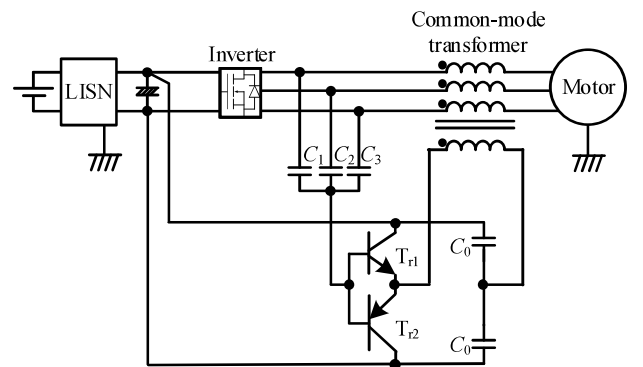
In recent years, significant research has been conducted on increasing power density in power converters using wide bandgap devices, such as SiC (silicon carbide) and GaN (gallium nitride)[1-2]. These devices achieve high-speed switching compared to Si devices, high-frequency drive, reduced volume of passive components, especially inductors, and high efficiency. However, high-speed switching leads to a steep potential voltage variation and a pronounced electromagnetic noise[3]. In addition, it is considered that the noise regulation frequency for inverters will be expanded to a low frequency from 150 kHz to 9 kHz. Therefore, electromagnetic noise suppression technologies will become increasingly important in the future.

Figure 1 shows conventional electromagnetic noise suppression methods. Figure 1 (a) is a passive CM filter that consists of a common-mode choke and a Y connection capacitor. The passive CM filters reduce electromagnetic noise in the frequency band above the cutoff frequency determined by the inductance and capacitance of the filter components. However, a low cutoff frequency is required to significantly reduce noise over a wide bandwidth. The passive CM filter with a low cutoff frequency increases the volume of the passive components and reduces power density.

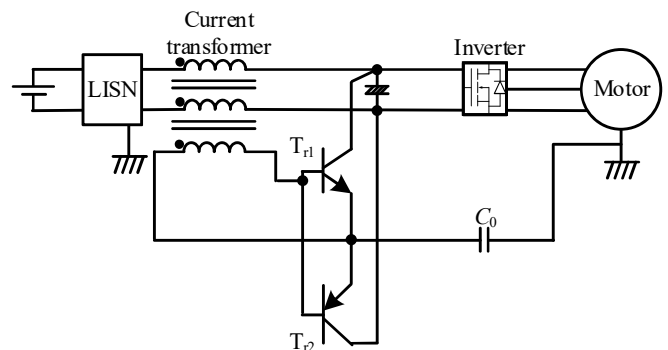
On the other hand, active common-mode noise cancellers (ACC) have been extensively researched to reduce the volume of the CM filter[5-6]. Figure 1 (b) is a voltage type ACC(Voltage Sensing Voltage Injection: VSVI), and Figure 1 (c) is a current type ACC (Current Sensing Current Injection: CSCI). The passive CM filters, including common-mode choke inductors and capacitors, are widely used to suppress electromagnetic noise, especially the CM noise.[4]



(a) Inverter circuit with passive filter



(b) Inverter circuit with VSVI



(c) Inverter circuit with CSCI

Fig.1. Conventional CM Filter

The ACC cancels the CM voltage or current with CM transformers or injecting amplifiers. Therefore, the ACC can reduce the circuit volume compared with the passive CM filters in the wide bandwidth design. There are two types of

ACC: voltage and current. The voltage type ACC adds the inverted waveform of the CM voltage to the output voltage of the inverter with a CM transformer. In contrast, the current type ACC injects the inverted waveform of the CM current, which is detected by a current transformer, to the grand wire of the load. The current type ACC has the advantage over the voltage type ACC in terms of high-power density because the current transformers are only required to detect the high-frequency component of the CM current.

The combination of an active EMI filter (AEF) and a modified LCL-LC harmonic suppression filter is proposed to replace the traditional EMI filter that has been proposed to solve the EMI issue without introducing additional system costs [11]. The final harmonic distortion analysis results of the grid-side current show the satisfactory harmonic attenuation performance of the modified LCL-LC filter, and the conducted EMI measurement results verify the superiority of the combination of the AEF and the modified LCL-LC filter. However, a transformer is used for CM current detection [11]. The transformer occupies a large portion of the circuit volume. The transformer increases the circuit volume.

A balanced feedforward current-sense current-compensation common-mode active electromagnetic interference filter has been proposed [12]. The proposed filter is applied to an L-C-L EMI filter for a 2.2 kW resonant inverter, and the CM noises are further reduced by 3 to 18 dB from 150 kHz to 10 MHz. The problem of the CM-to-differential mode noise transformation due to an unbalanced filter structure is also investigated by the measurements using a vector network analyzer. However, [12] uses transformers and transistors in the filter, which reduces the noise reduction effect at high frequencies.

This paper proposes the current type ACC with Rogowski coils, which is used as the CM current detection in order to minimize the volume of the current transformer. The advantage of the Rogowski coil is that the primary winding becomes just one turn. Moreover, the Rogowski coil can easily increase the number of turns on the secondary side. Consequently, the Rogowski coil is smaller than that of the normal current transformer for CM current detection. The target frequency range of the CM current reduction is from 150 kHz to 30 MHz based on the guidelines of the CISPR standard. The new contribution of this paper is that the proposed design method reveals the number of turns and the detection resistance of the Rogowski coil to respect the CISPR standard.

The paper is organized as follows: firstly, The circuit configuration of the current type ACC is described. Secondly, the design method of a current type ACC according to the reduction gain of the conducted emission voltage. Finally, the proposed design method is evaluated by the experiment and discussed in terms of the noise reduction effect of the proposed circuit.

II. CIRCUIT CONFIGURATION

Figure 2 shows the circuit diagram of the proposed current type ACC. The current type ACC includes the CM current detection using a Rogowski coil, a non-inverting amplifier circuit, a voltage regulator for the amplifier, and a coupling capacitor C_0 . The CM current is detected by the Rogowski coil. The detected current is converted to a voltage by a resistor on the secondary side of the Rogowski coil. The non-inverting

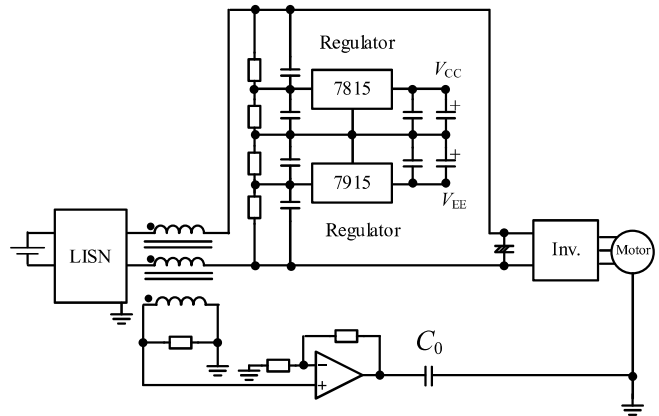


Fig.2. Conflagration of current type

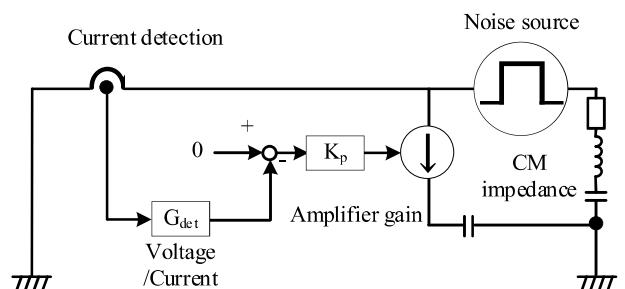


Fig.3. Equivalent block diagram of ACC in common mode circuit.

amplifier circuit amplifies the voltage value and injects a compensation current between the motor and the grand wire via the coupling capacitor.

Figure 3 shows a block diagram of the current type ACC in a common-mode equivalent circuit. The current type ACC is configured as a feedback control system for the CM current flowing into the power supply side. It suppresses the CM current by proportional control with a command value of 0 A. The noise reduction effect depends on the proportional gain, determined by the detection current-detection voltage ratio and amplifier gain.

The conducted emission voltage suppression will be insufficient when the frequency range for each of the circuits (current detection section using Rogowski coils, amplification section using operational amplifiers, and compensation current injection section) that make up the current type ACC is low compared to the compensation frequency band. The devices and other components that have a significant influence on the respective frequency bands are described below.

A. Amplifier part

The amplifier section in the conventional ACC often uses a push-pull voltage follower circuit, limiting the bandwidth [7-10]. However, high-voltage transistors connected directly to the DC bus have a low-frequency response. Therefore it is difficult to achieve high bandwidth ACC. This paper applies a non-inverting amplifier circuit using a high-performance current feedback operational amplifier to increase the ACC bandwidth. The power supply part of the amplifier is supplied with a DC bus voltage divided by a capacitor and stepped down to 15 V by a series regulator.

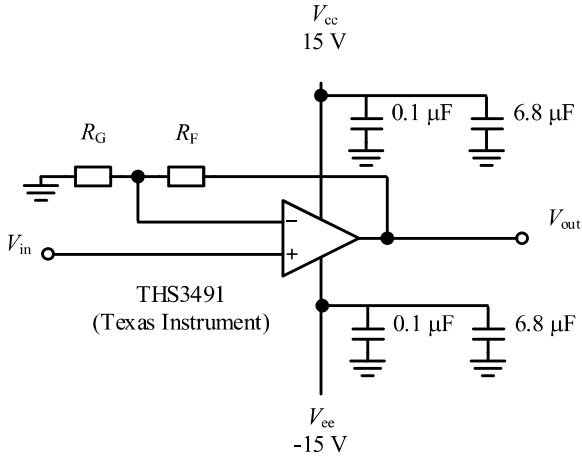


Fig.4. Noninverting amplifier circuit.

Table 1. Operational Amplifier Resistance.

Gain	$R_G(\Omega)$	$R_F(\Omega)$
2	2100	2100
5	200	798
10	76.7	704
20	29.4	564

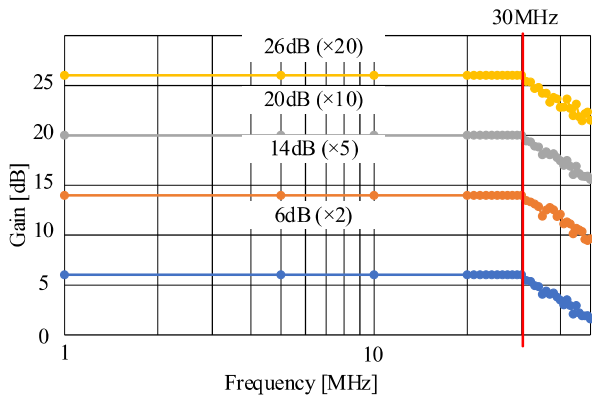


Fig.5. Gain characteristics of amplifier only.

Figure 4 shows a non-inverting amplifier circuit using the current feedback operational amplifier. The amplifier in the ACC requires a very wide frequency range and a large output current. As a result, an output current feedback type amplifier (THS3491 (Texas Instruments)), which operates with a maximum bandwidth of 900 MHz in ideal state operation, is selected. Table 1 shows the amplifier circuit listed in the datasheet, showing the optimum combination of resistors to obtain the desired gain. The amplifier circuit for each gain was created using the resistor values in this table.

Figure 5 shows the frequency characteristics of the non-inverting amplifier circuit when the resistors described in the data sheet are used. The figure shows that all gains are constant up to 30 MHz in the amplifier circuit alone.

Figure 6 shows the circuit configuration in which the frequency-gain characteristics of the amplifier of the current type ACC are measured. The voltage applied to the load was measured when a sinusoidal voltage from 100 kHz to 30 MHz was input to the amplifier by a function generator. The load was connected in series with a 50 Ω resistor and a 1 μ F capacitor. In actual operation as ACC, the return line of the

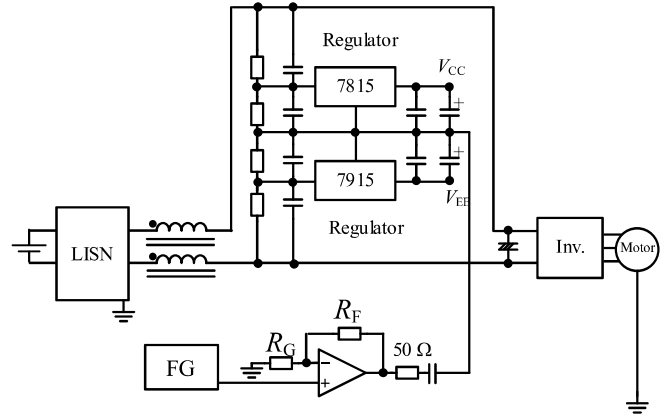


Fig.6. Measurement circuit configuration of ACC frequency characteristics.

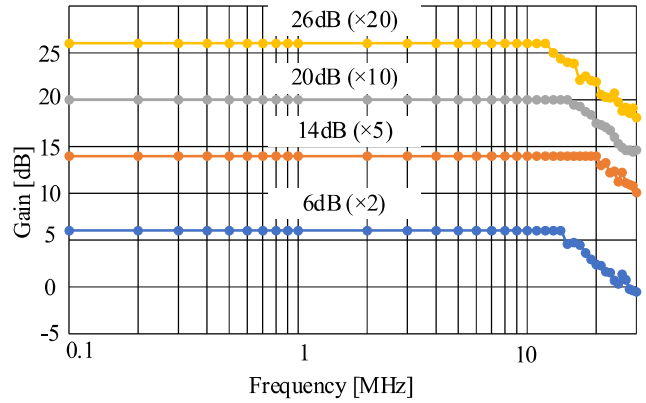


Fig.7. Gain characteristics of ACC circuit only.

amplifier is the common mode circuit of the motor and inverter. However, the load is connected to the reference point (DC bus mid-point) of the operational amplifier power generation circuit, which is composed of a capacitor voltage divider and regulator.

Figure 7 shows the measured frequency-gain characteristics of the ACC circuit. At high-frequency regions, the effect of the wiring inductance increases. The connection to the circuit increases the wiring inductance and reduces the gain characteristics of the amplifier. However, the amplifier operates with the designed gain up to 14 MHz at two times gain, 20 MHz at five times gain, 15 MHz at ten times gain, and 12 MHz at 20 times gain.

B. Compensation current injection section

The compensation current output by the operational amplifier is injected into the ground wire via the coupling capacitor C_0 . The electromagnetic noise must be reduced to the specified value determined by the CISPR for 150 kHz to 30 MHz. Thus the capacitance of the coupling capacitor should be selected so that the impedance of the capacitor at 150 kHz is sufficiently low. In this paper, the value is set to 1 μ F, approximately 1 Ω at 150 kHz

C. CM current detection section

Current transformers (CT) are widely used in the current-type ACCs to detect CM currents, as CT uses a magnetic core and detects CM currents according to the ratio of primary and secondary windings, making it easy to design a high detection

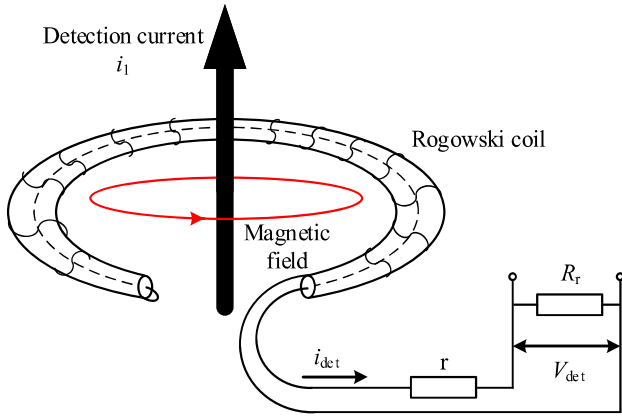


Fig.8. Rogowski coil conceptual diagram.

gain. However, the number of primary windings and magnetic cores used limit the frequency band that is detected. For this reason, this paper applies the Rogowski coil to broaden the bandwidth of the detection unit of the ACC and expand the reduction range of the conducted emission voltage. The detailed design of the Rogowski coil is described in the next chapter.

III. DESIGN OF ROGOWSKI COILS

Figure 8 shows the principle diagram of a Rogowski coil. The coupling between the primary winding (the winding through which the CM current flows) and the secondary winding (the Rogowski coil) does not necessarily have to be high when applying a Rogowski coil. The CISPR defines the allowable conducted emission voltage in the band between 150 kHz and 30 MHz; the evaluation of the characteristics of the voltage output to the detected current at the detection unit is carried out in the band between 150 kHz and 30 MHz. The evaluation of the characteristics of the output voltage concerning the detected current of the detection unit is carried out in the 150 kHz to 30 MHz band.

Figure 9 shows the design flow of the Rogowski coil. In the design of the Rogowski coil, the cutoff frequency must be designed sufficiently low compared to 150 kHz for the ACC to have a sufficient reduction effect in all conducted noise measurement frequency bands. In addition, the detection current-to-detection voltage ratio should be designed to be high to increase the noise reduction effect of the ACC. The average flux density B at the cross-section of the Rogowski coil is expressed as

$$B = \frac{\mu(i_1 + N i_2)}{2\pi r_R} \dots\dots\dots(1),$$

where i_1 is the CM current to be measured, i_2 is the current flowing in the Rogowski coil, N is the number of coil turns, and r_R is the radius of the circle formed by the Rogowski coil.

The electromotive force V induced at both ends of the Rogowski coil is expressed as

$$V = -N \frac{\partial \Phi}{\partial t} = -\frac{\mu_0 N S_R}{2\pi r_R} \frac{\partial}{\partial t} (i_1 + N i_2) \dots\dots\dots(2)$$

where S_R is the cross-sectional area of the Rogowski coil. If the output resistance connected to the secondary side is R and the parasitic resistance of the Rogowski coil is r , the

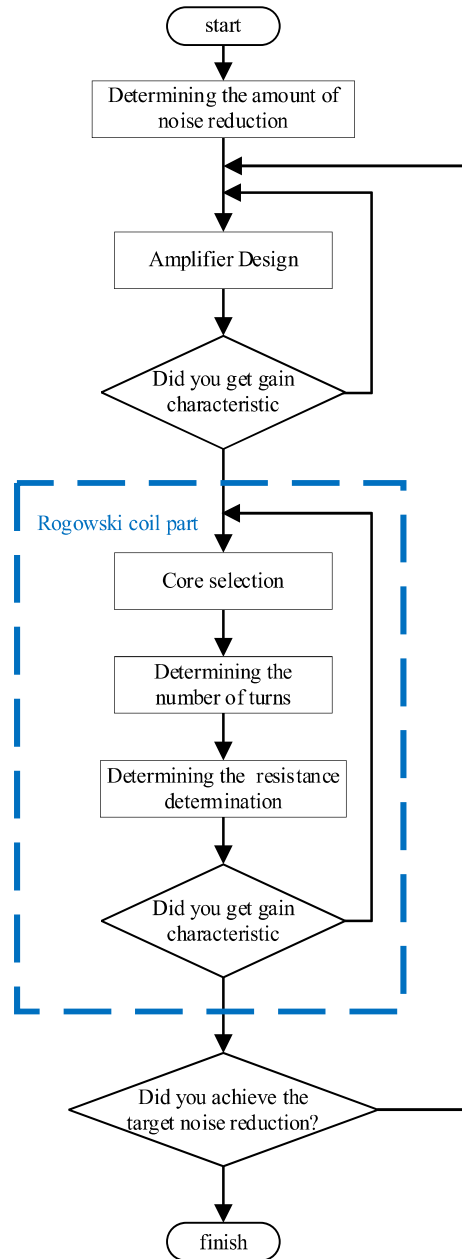


Fig.9. Design flow of ACC

relationship between the power V at both ends of the Rogowski coil and the secondary side current i_2 is expressed by the following equation.

$$V = (R+r)i_2 \dots\dots\dots(3)$$

The self-inductance L of the Rogowski coil is expressed by the following equation

$$L = \frac{\mu_0 N^2 S_R}{2\pi r_R} \dots\dots\dots(4)$$

Substituting (3) and (4) into (2), the differential equation concerning voltage is obtained from the following differential equation concerning voltage

$$\frac{dV}{dt} + \frac{R+r}{L} V = -\frac{R+r}{N} \frac{di_1}{dt} \dots\dots\dots(5)$$

$$V = -\frac{j\omega \frac{L}{N} i_1}{\frac{R+r}{L} + j\omega} \dots\dots\dots(6)$$

where $(R + r)/L$ is the dimension of angular frequency, so the cutoff frequency is expressed by the following equation

$$f_L = \frac{R + r}{2\pi L} \dots\dots\dots (7)$$

The output is the voltage at both ends of the external resistor R when used as a detector. The voltage at both ends of the external resistor R , $V_{observe}$, is the voltage divider between R and r and is expressed by the following equation.

$$|V_{observe}| = \frac{\frac{f}{f_L}}{\sqrt{1 + \frac{f^2}{f_L^2}}} \frac{R}{N} |i_c| \dots\dots\dots (8)$$

First, the window area of the core is determined by the current flowing in the main circuit. The cross-sectional area of the wiring, A_w , is expressed by the following equation, assuming a DC i_{dc} and winding current density J .

$$A_w = \frac{i_{dc}}{J} \dots\dots\dots (9)$$

The load motor is 200 V, 750 W. The DC side current at rating is assumed to be 3.5 A, and the winding current density is designed to be 4 A/mm². Since a maximum current of 3.5 A flows in the circuit, the cross-sectional area of the wiring needs to be at least 0.875 mm² according to formula (9), taking into account the fact that two wires pass through to detect the CM current, the wiring covering, etc. Furthermore, a core with an inner diameter of 33.2 mm² was selected to allow a margin, taking into account the ease of winding the secondary winding and the availability of cores.

Next, the number of turns of the Rogowski coil is determined. To detect CM currents from the low-frequency range, the bandwidth of the Rogowski coil must be low, and the number of turns must be increased to increase the inductance from equation (7). Therefore, the magnetic path length of the core selected this time was 56 mm, and 120 turns of 0.4 mm enameled wire were used. For the core material, a ferrite core with a magnetic permeability μ_r of 450 at 950 kHz was selected because of the need to design a high self-inductance.

Finally, the detection resistor R is designed. The detection resistor was set to 2400 Ω so that the cutoff frequency calculated by equation (7) is sufficiently low relative to the measurement range of 150 kHz, and the detection gain calculated by equation (8) is larger. The design with the parameters determined above resulted in a cutoff frequency of 17 kHz and a detection current-to-detection voltage ratio of 20 times, which were sufficiently low compared to the cutoff frequency of 150 kHz so that the designed Rogowski coil is used as a CM current detection unit. The designed Rogowski coil is used above the CISPR standard of 150 kHz.

Figure 10 shows the photo of the created Rogowski coil. Table 2 shows the parameters of the Rogowski coil. The outer shape of the Rogowski coil, including the windings, is 26 mm, and its weight is 28.6 g. The Rogowski coil in the detection section detects the CM current flowing in the main circuit, converts the current voltage on the secondary side, and outputs it to the amplifier.

Figure 11 shows the characteristics of the detected current-detected voltage ratio of the Rogowski coil as a function of frequency change. The measurement results show that a detection gain of 25dB was obtained for the Rogowski coil.

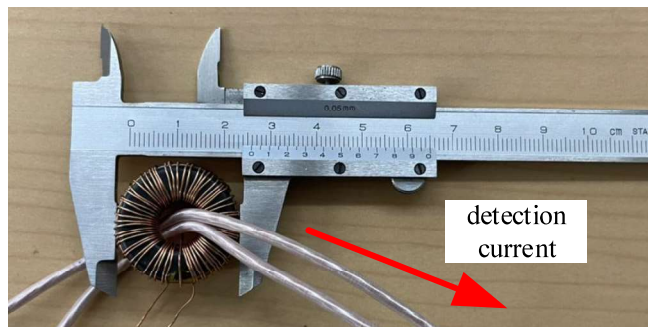


Fig.10. Rogowski coil.

Table 2. Parameters of Rogowski coil.

Core size (mm)	25
Number of turns	120
Detection resistance(Ω)	2400
Inductance value (mH)	2.16
Cutoff frequency (kHz)	20
Detection gain (dB)	25

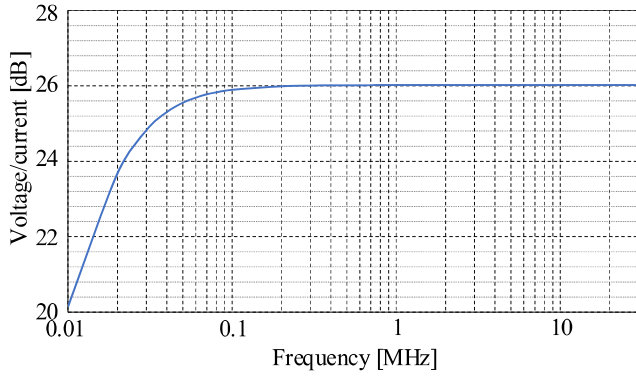
However, an error of 3.8% occurred due to changes in magnetic permeability and differences in wiring impedance compared to the design value. The cutoff frequency was 20 kHz, which is sufficiently small compared to 150 kHz. The detection gain is constant up to 30 MHz, indicating that the CM current detection unit is used in the noise measurement range from 150 kHz to 30 MHz with the designed detection gain.

IV. EXPERIMENTAL RESULTS

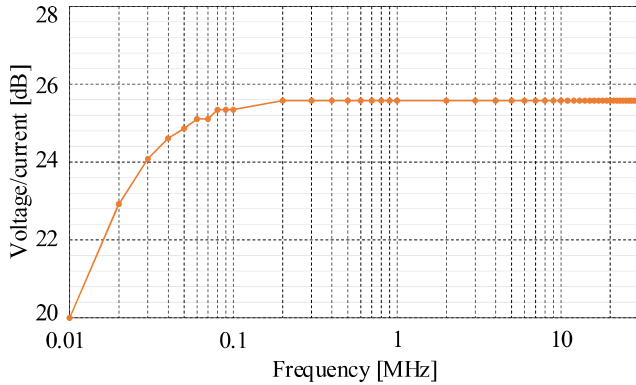
Figure 12 shows the measurement layout of a conducted emission voltage. As the layout for measuring conducted emission voltages that are defined by CISPR 16, comparative measurements were carried out under conditions close to the defined measurement method. The inverter and the induction motor were placed 40 cm from the ground surface on support. A spectrum analyzer measures an electromagnetic conducted emission voltage reaching the LISN as the conducted emission voltage.

Figure 13 shows the CM current waveforms under the experimental measurements. Figure 13 (a) shows the CM current waveform without ACC. Figure 13 (b) shows the waveforms of the measured results of the CM current between inverter and motor, between ACC and inverter, and between ACC and power supply when the amplifier gain is multiplied by 20. The CM current resonating at 3.3 MHz flows to the grand wire at a maximum of 400 mA without the ACC. On the other hand, CM current flows through the motor, amplifier, amplifier power supply, and inverter paths, reducing the CM current flowing to the LISN side with ACC.

Figure 14 shows the comparison of the measured conducted emission voltage with and without ACC. The conducted emission voltage was measured under four conditions of the amplifier gain with ACC: the amplifier gain is two times, five times, ten times, and 20 times. The conducted emission voltage of 90.7dB is measured at 2.7 MHz without ACC. The conducted emission voltage decreased in all bands from 150 kHz to 30 MHz with ACC. From this, the current type ACC with the designed Rogowski coil is effective for noise reduction in all frequency bands of the measurement



(a) Design value.



(b) Measured value.

Fig.11. Rogowski coil frequency characteristics.

range. Also, when the ACC was operated, a reduction of 17.9dB was obtained at 2.7 MHz when the amplifier gain was two times, 24.4dB at five times, 27.0dB at ten times, and 35.9dB at 20 times, confirming that the noise reduction effect is improved by increasing the amplifier gain and designing a higher gain of the ACC. Figure 12 (d) shows the conducted emission voltage when the amplifier gain is increased by 20 times and the conducted emission voltage limits specified in CISPR12. The figure shows that the conducted emission voltage reduced by ACC exceeds the specified value defined by CISPR at around 3 MHz.

To further improve the noise reduction effect of ACC, the resistance value of the non-inverting amplifier circuit was changed, as shown in Table 3.

Figure 15 shows the results of the frequency response measured at 30 times the gain with the circuit configuration shown in Fig. 6. The figure shows that the gain is lower at 10 MHz and above. However, the gain is higher than 20 times in all frequency bands, indicating that the noise reduction of ACC is expected to be higher.

Figure 16 shows the measured conducted emission voltage when the amplifier gain is increased to 30 times. The figure shows that the amount of noise reduction increased in all frequency ranges compared to when the amplifier gain was increased to 20 times and that the CISPR-specified values, which were exceeded when the amplifier gain was increased to 20 times, were satisfied.

V. CONCLUSION

This paper proposed a Rogowski coil design for use in the detection section of a current type ACC. The cutoff frequency

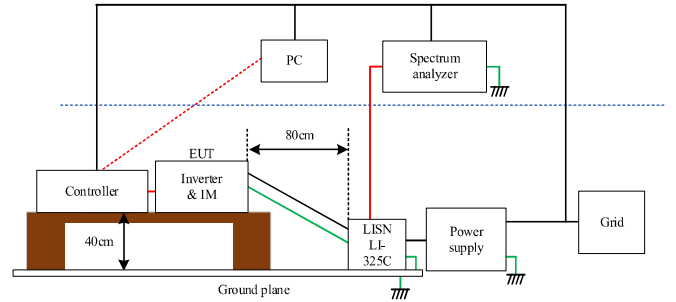
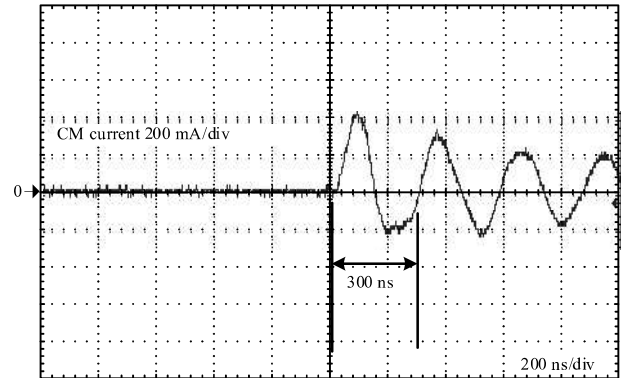
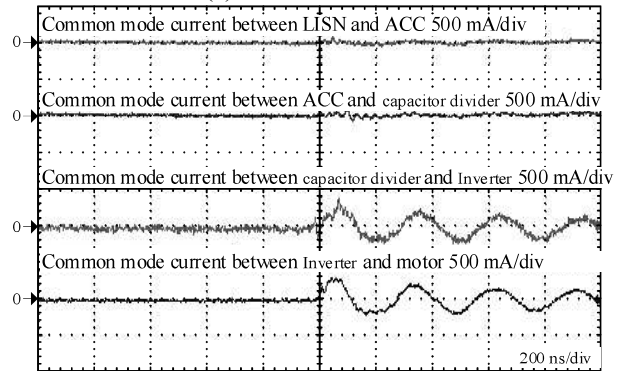


Fig.12. EMI evaluation layout.



(a) Without ACC.

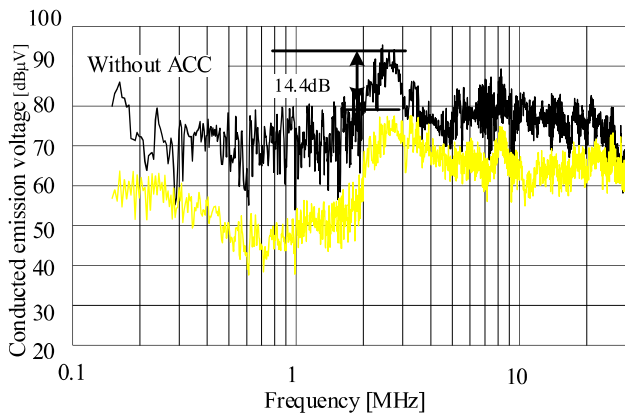


(b) With ACC.

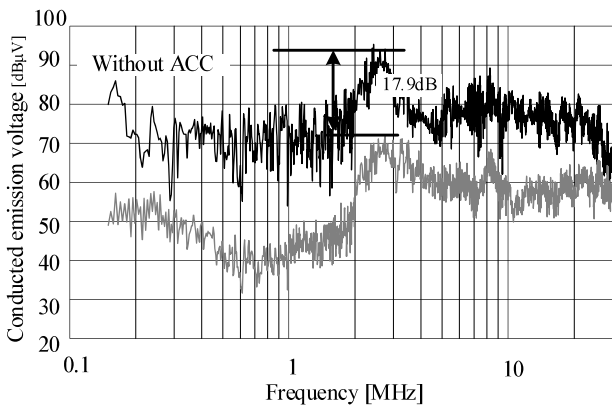
Fig.13. CM current waveforms.

was designed to be sufficiently low compared to 150 kHz. It was confirmed that the noise reduction effect of ACC was expanded by designing a wider frequency band. The experimental results demonstrated a maximum noise reduction of 39.0dB μ V in the frequency range of 150 kHz to 30 MHz, which is the frequency band specified by CISPR. In addition, the conducted emission voltage was reduced more by increasing the ACC gain, which is calculated by the ratio of the detected current to the voltage of the Rogowski coil and the amplifier gain. The experimental results show that the noise reduction effect was confirmed in all frequency bands between 150 kHz and 30 MHz, the frequency band specified in the CISPR, and that the Rogowski coil designed in this study is sufficiently effective in reducing conducted noise.

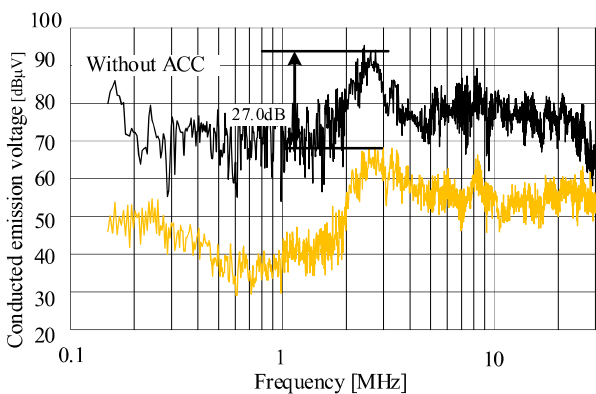
In the future, the current-type ACC will be designed to achieve arbitrary noise reduction through a more detailed design.



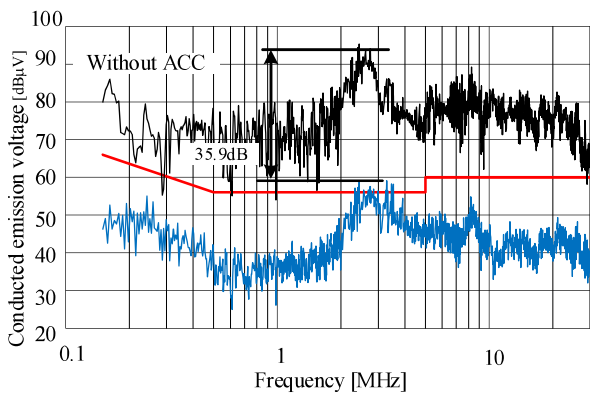
(a) Amp gain: two times



(b) Amp gain: five times



(c) Amp gain: ten times



(d) Amp gain: 20 times

Fig.14. Conducted emission voltage.

Table 3. Operational Amplifier Resistance. (Gain:30 times)

Gain	$R_G(\Omega)$	$R_F(\Omega)$
20	29.4	564
30	24	680

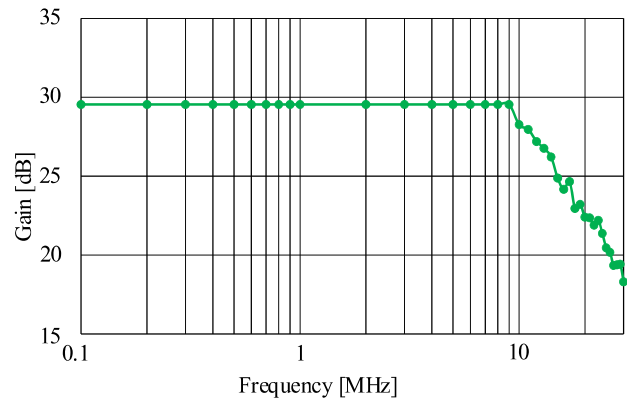


Fig.15. Amplifier gain characteristics. (Gain: 30 times)

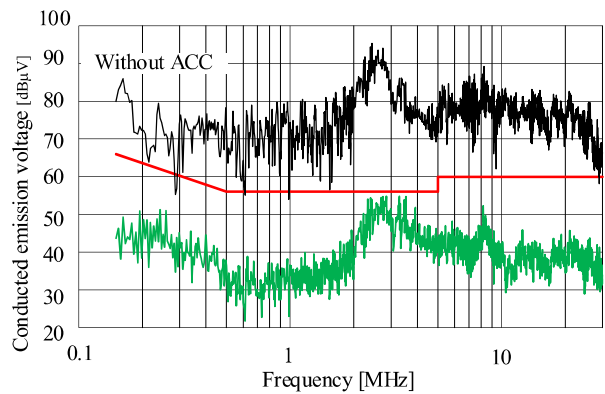


Fig.16. Conducted emission voltage. (Gain: 30 times)

REFERENCES

- [1] Ikuya Sato, Takaaki Tanaka, Motohito Hori, Ryouji Yamada, "High Power Density Inverter Utilizing SiC MOSFET and Interstitial Via Hole PCB for Motor Drive SystemSiC", IEEJ, Vol. 140, No. 7, pp.526-533 (2020)
- [2] Junji Kondoh, Tsutomu Yatsuo, Itaru Ishii, Kazuo Arai, "Estimation of Converters with SiC Devices for Distribution Networks," IEEJ Trans. On Industry Applications, Vol. 126, No. 4, pp. 480-488 (2006).
- [3] Kenji Sato, Hirokazu Kato, Takafumi Fukushima, "Development of SiC Applied Traction System for Next-Generation Shinkansen High-Speed Trains," IEEJ Journal of Industry Applications, Vol. 9, No. 4 pp. 453-459 (2020).
- [4] Shin-Ichiro Hayashi, Keiji Wada, Implementation of a Gate Drive Circuit for Reducing Switching Loss and Surge Voltage, IEEJ, Vol. 136, No. 10, pp. 791-797 (2016)
- [5] S. Takahashi, K. Wada, H. Ayano, S. Ogasawara, T. Shimizu, "Review of Modeling and Suppression Techniques for Electromagnetic Interference in Power Conversion Systems," IEEJ Trans. On Industry Applications, Vol. 11, No. 1, pp. 7-19 (2022).
- [6] Kazuhiro Umetani, Takahiro Tera, Kazuhiro Shirakawa, "A Magnetic Structure Integrating Differential-mode and Common-mode Inductors with Improved Tolerance to DC Saturation," IEEJ Journal of Industry Applications, Vol. 4, No. 3, pp. 166-173 (2015)
- [7] Satoshi Ogasawara, Hideaki Fujita, Hirofumi Akagi, Modeling and Analysis of High-Frequency Leakage Currents Caused by Voltage-Source PWM Inverters, IEEJ, Vol.115, No.1 号, pp77-83(1995)
- [8] Isao Takahashi, Akihiro Ogata, Hidetoshi Kanazawa, Atsuyuki Hiruma, "Active EM1 Filter for Switching Noise of High-Frequency Inverters" IEEE (1997)

- [9] Satoshi Ogasawara, Hideki Ayano, and Hirofumi Akagi, "An Active Circuit for Cancellation of Common -Mode Voltage Generated by a PWM Inverter" IEEE TRANSACTIONS ON POWER ELECTRONICS, VOL.13, NO.5,pp835 -841 (1998)
- [10] Satoshi Ogasawara, Hideki Ayano, Hirofumi Akagi, Active Cancellation of the Common-Mode Voltage Produced by a Voltage-Source PWM Inverter, IEEJ, Vol.117, No.5 号, pp565 -571(1997)
- [11] Shiqi Jiang, Yitao Liu, Member, Weihua Liang, Jianchun Peng, and Hui Jiang, "Active EMI Filter Design With a Modified LCL-LC Filter for Single-Phase Grid-Connected Inverter in Vehicle-to-Grid Application" IEEE TRANSACTIONS ON POWER ELECTRONICS, VOL.68, NO.11,pp639 -650 (2019)
- [12] Dongil Shin, Sangyeong Jeong, Youngjin Baek, Chansoo Park, Gwigeun Park, and Jinguok Kim, "A Balanced Feedforward Current-Sense Current-Compensation Active EMI Filter for Common-Mode Noise Reduction" IEEE TRANSACTIONS ON POWER ELECTRONICS, VOL.62, NO.2,pp386 -397 (2020)